Electronic Supplementary Material (ESI) for Environmental Science: Nano.

Electronic Supplementary Information

Table S1. Chemical structures of FQs being used as model organic pollutant

FQs	Structure	λ_{max} (nm)	MW (g/mol)	Solubility (g/L)	pKa	Existing
Ofloxacin (OFX)	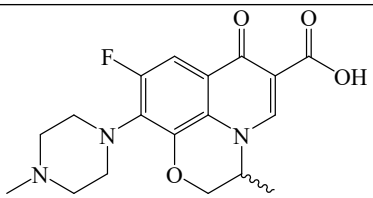	291	361.36	10.8	pKa_1=6.1; pKa_2=8.28	OFX^+, OFX^- $OFX^{Zwitterion}$
Levofloxacin (LFX)	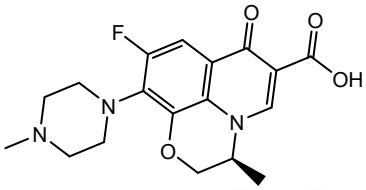	297	361.36	1.5	pKa_1=6.24; pKa_2=8.74	LFX^+, LFX^- $LFX^{Zwitterion}$
Ciprofloacin (CFX)	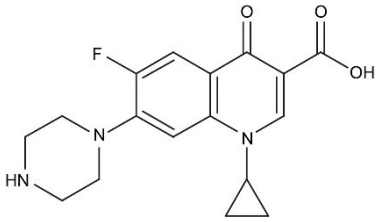	278	331.35	1,0	pKa_1=6.09; pKa_2=8.62	CFX^+, CFX^- $CFX^{Zwitterion}$

Table S2. Intermediate product of ofloxacin in BIZ/$Na_2S_2O_8$/Vis system identified by LC-ESI-QTOF-MS

Compound	m/z	Molecular formula	Molecular structure Retention time
M_1	393	$C_{18}H_{20}FN_3O_6$	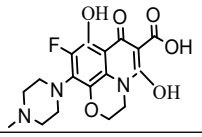
M_2	347	$C_{17}H_{18}FN_3O_4$	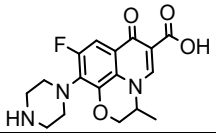
M_3	329	$C_{17}H_{19}N_3O_4$	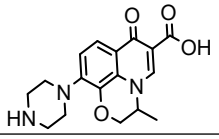
M_4	277	$C_{13}H_{10}FN_2O_4$	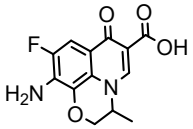
M_5	231	$C_{12}H_{11}FN_2O_2$	
M_6	256	$C_{10}H_7FNO_6$	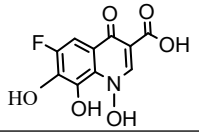
M_7	238	$C_{10}H_8NO_6$	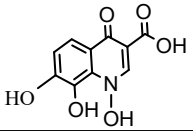
M_8	312	$C_{17}H_{18}N_3O_3$	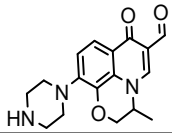
M_9	261	$C_{13}H_{10}FN_2O_3$	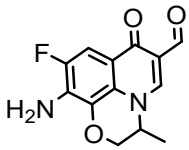
M_{10}	212	$C_{12}H_{11}N_2O_2$	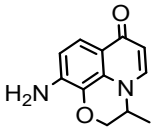
M_{11}	224	$C_{10}H_6FNO_4$	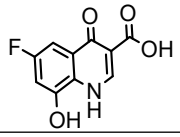

M_{12}	206	$C_{10}H_7NO_4$	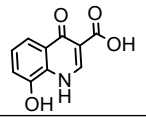
M_{13}	234	$C_{12}H_{11}FN_2O_2$	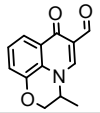
M_{14}	198	$C_9H_7FN_2O_2$	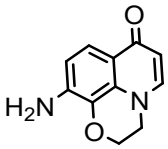
M_{15}	194	$C_9H_7FN_2O_2$	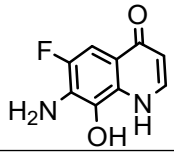
M_{16}	208	$C_{10}H_6FNO_3$	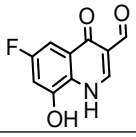
M_{17}	161	$C_9H_7NO_2$	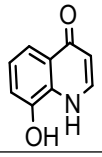
M_{18}	216	$C_{12}H_{12}N_2O_2$	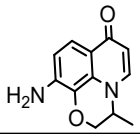
M_{19}	177	$C_{12}H_{12}N_2O_2$	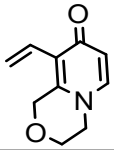
M_{20}	176	$C_9H_8N_2O_2$	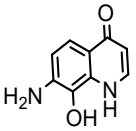
M_{21}	165	$C_8H_5O_4^-$	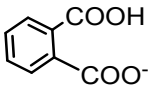
M_{22}	137	$C_7H_6O_3$	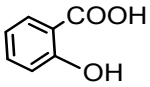
M_{23}	110	$C_6H_6O_2$	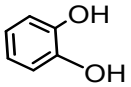

M_{24}	93	C_6H_7N	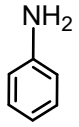
M25	116	$C_4H_4O_4$	HOOCCH=CHCOOH
M_{26}	90	$C_2H_2O_4$	HOOC-COOH
M_{27}	86	$C_4H_6O_2$	CH_2=CHCH_2COOH
M_{28}	84	$C_4H_4O_2$	CH≡CCH_2COOH
M_{29}	70	C_4H_6O	CH_2=CHCH_2CHO
M_{30}	68	C_4H_4O	CH≡CCH_2CHO
M_{31}	56	C_3H_4O	CH_2=CHCHO

Figure S1. Procedure for synthesis of BIZ heterojunction

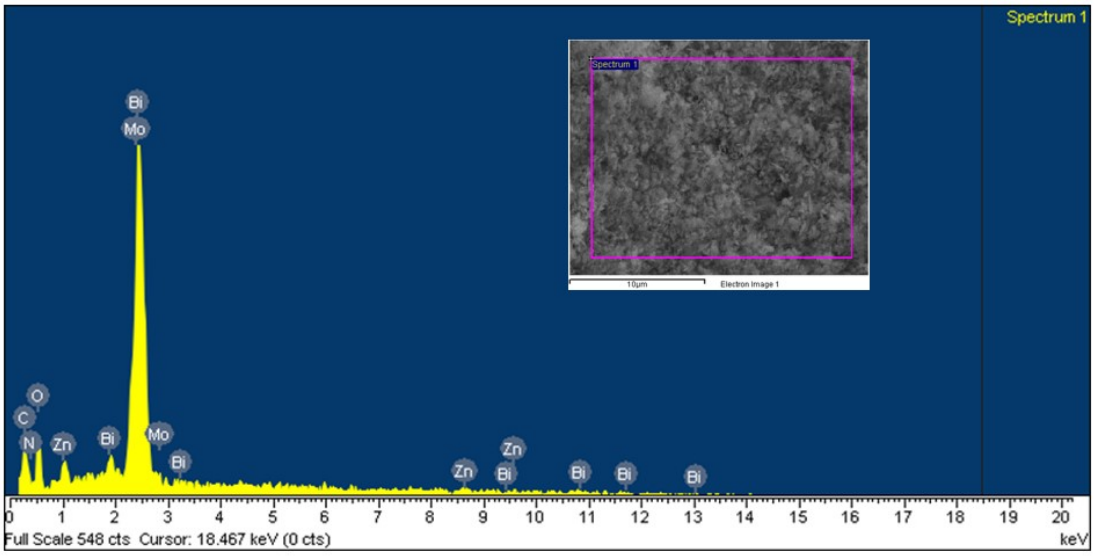

Figure S2. The EDX result of the BIZ heterojunction

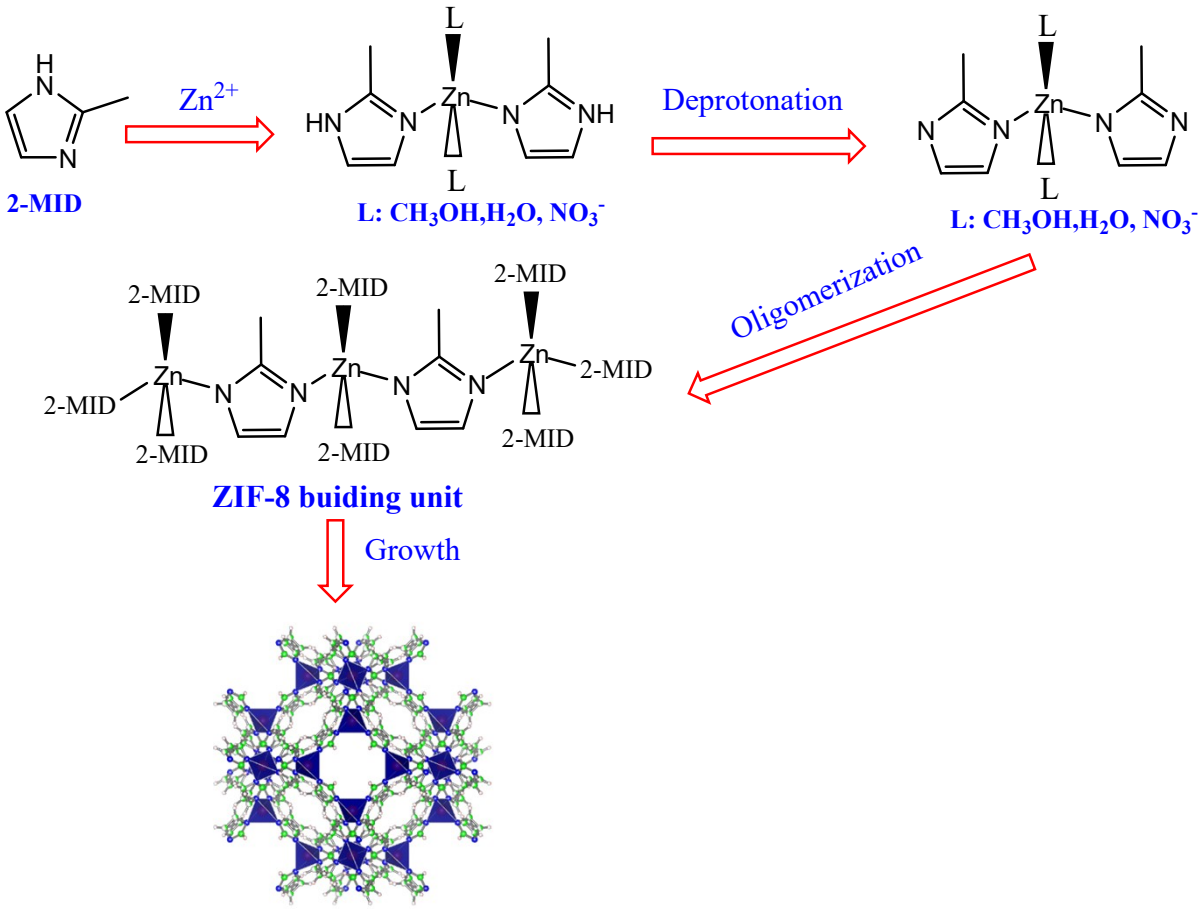

Figure S3. Proposed mechanism for the formation of ZIF-8 material

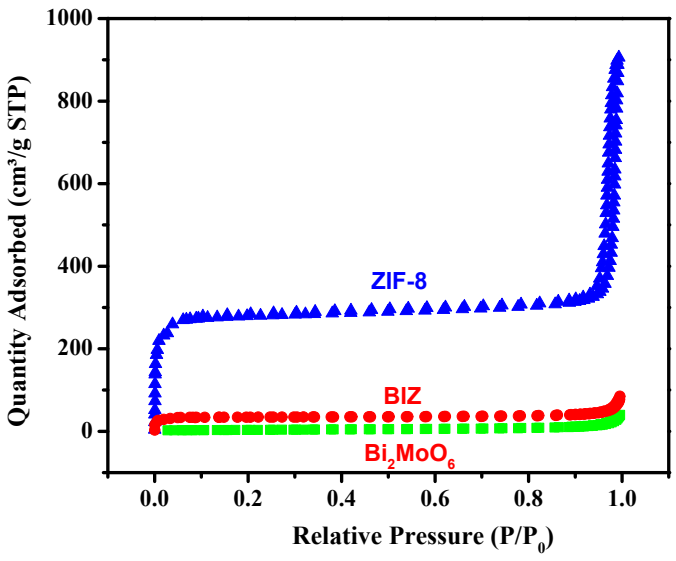

Figure S4. The N_2 adsorption-desorption isotherms of Bi_2MoO_6, ZIF-8, and BIZ materials

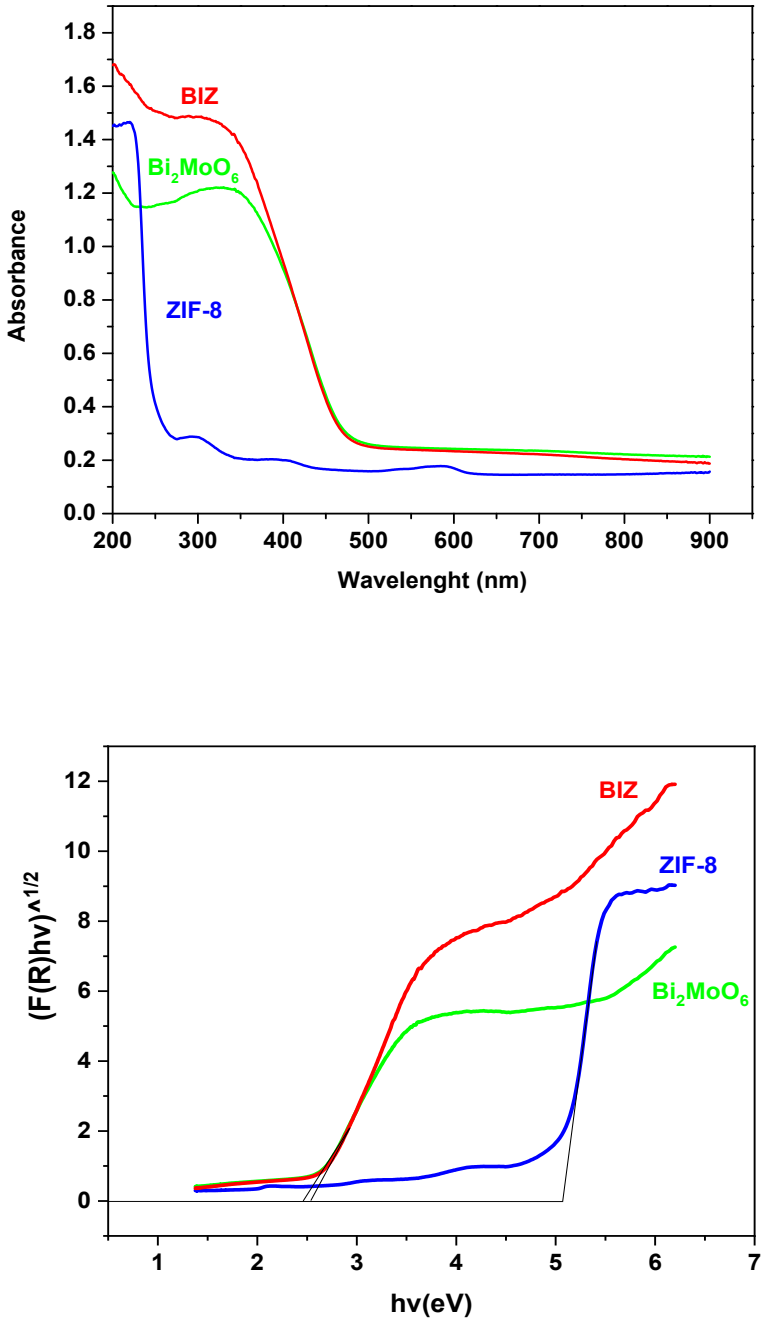

Figure S5. UV-Vis DRS spectra of Bi_2MoO_6, ZIF-8, and BIZ materials

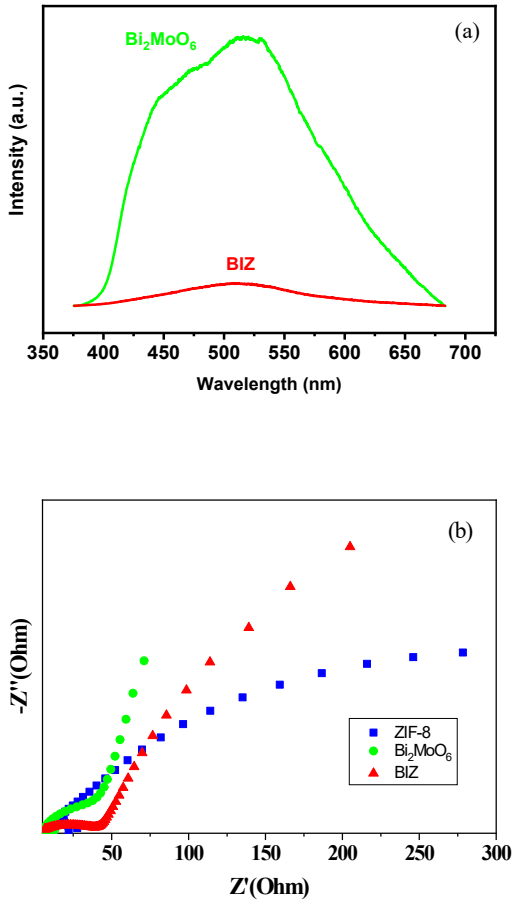

Figure S6. (a) PL spectra of pure Bi_2MoO_6 and BIZ heterojunction, and (b) EIS Nyquist plots of ZIF-8, Bi_2MoO_6, and BIZ

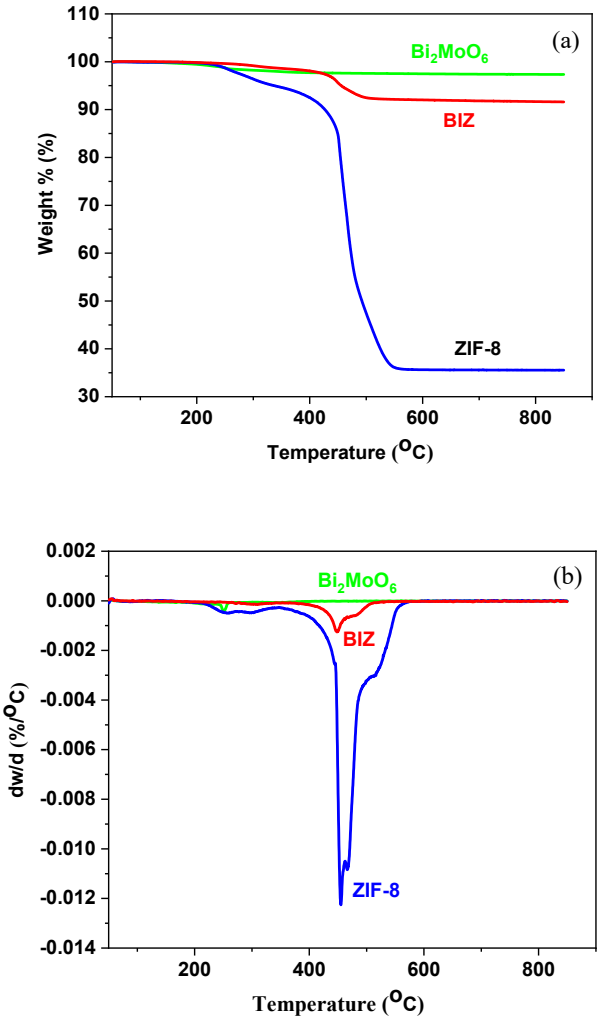

Figure S7. (a) TG and (b) DTG results of Bi_2MoO_6, ZIF-8, and BIZ materials

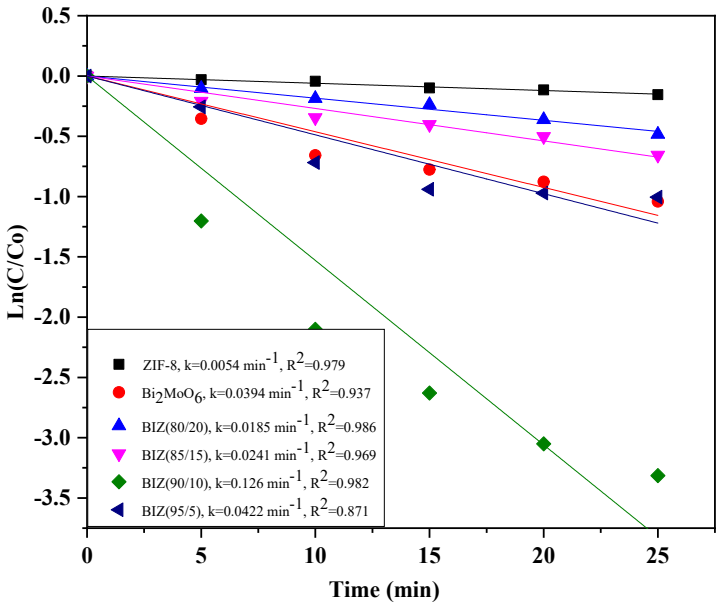

Figure S8. Photocatalytic decomposition rates of OFX by different BIZ materials (n = 3)

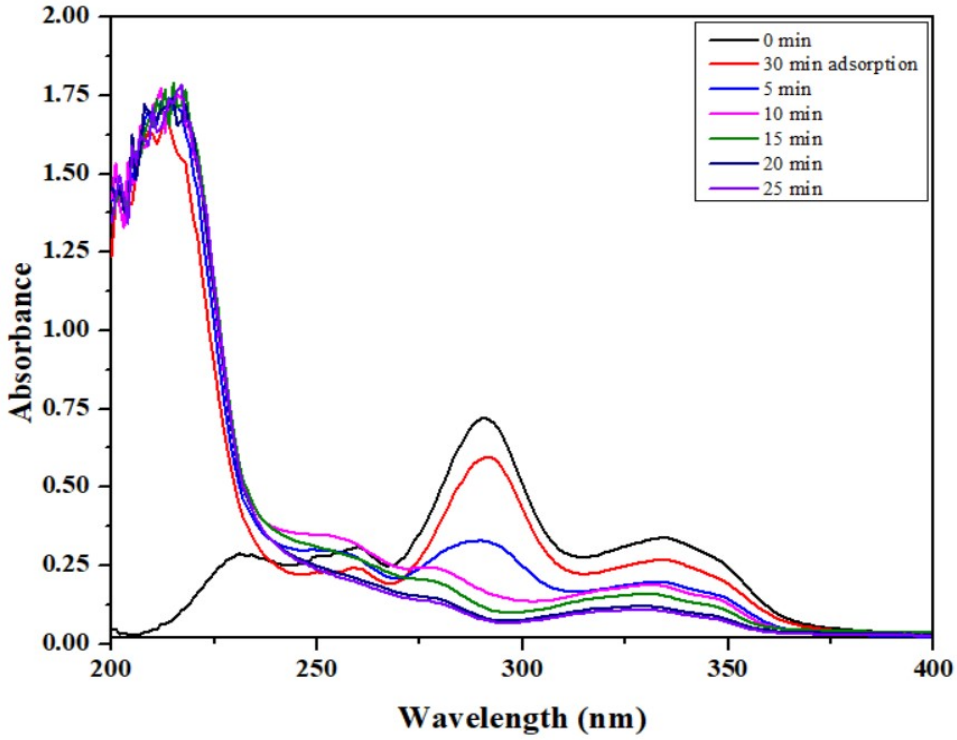

Figure S9. UV-Vis spectra of OFX during 30 min of adsorption and then 25 min of photocatalysis

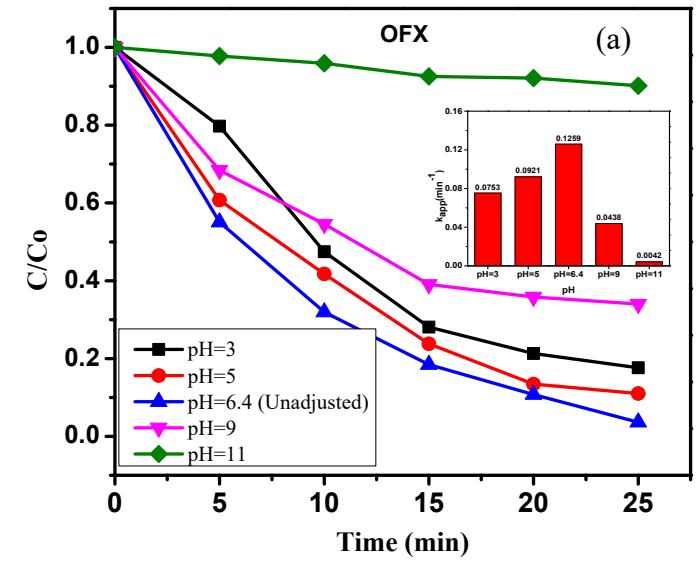
OFX
(a)
C/Co
Time (min)
pH=3
pH=5
pH=6.4 (Unadjusted)
pH=9
pH=11
0.0753
0.0921
0.1259
0.0438
0.0042
pH

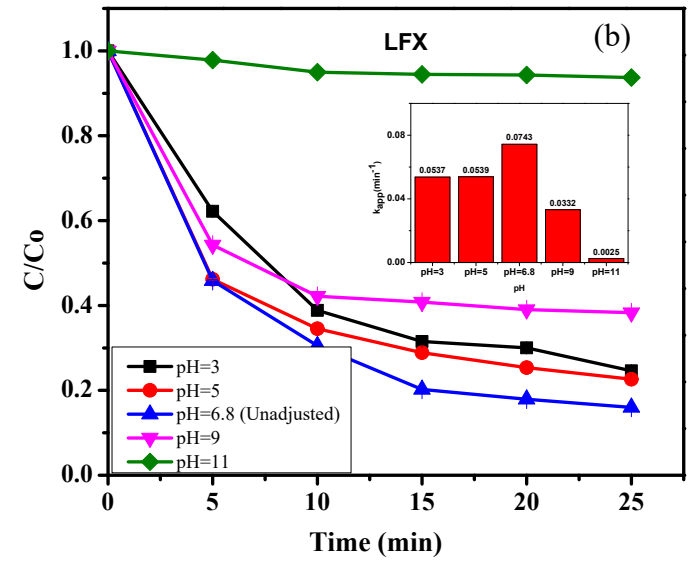
LFX
(b)
C/Co
Time (min)
pH=3
pH=5
pH=6.8 (Unadjusted)
pH=9
pH=11
0.0537
0.0539
0.0743
0.0332
0.0025
pH

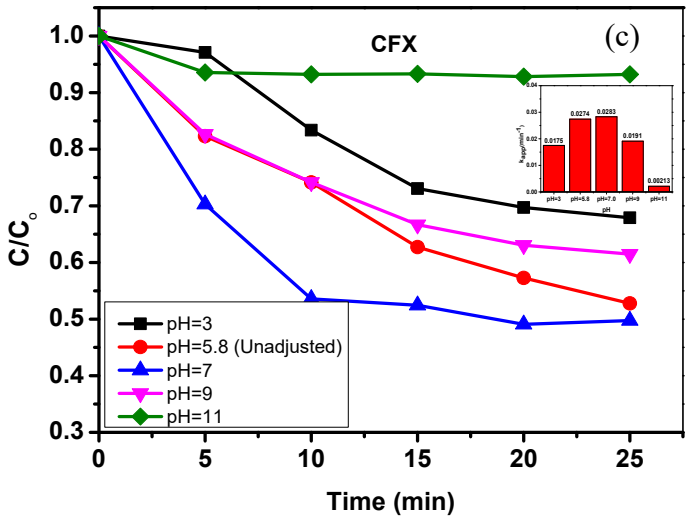

Figure S10. Effects of initial pH on the photocatalytic removal efficiency of (a) OFX, (b) LFX, and (c) CFX (Insets are the pseudo-first-order reaction rate constants at different pH)

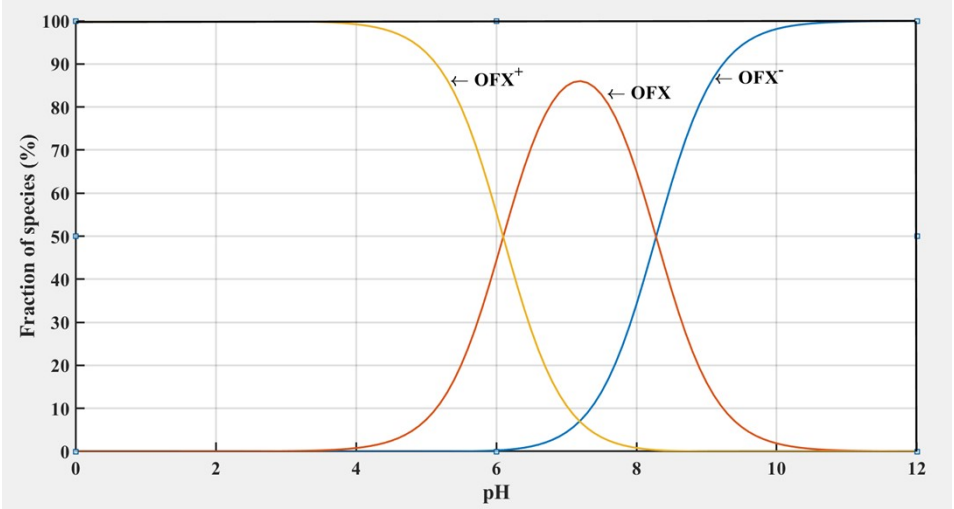

Figure S11. Specification of ofloxacin as a function of pH value in aqueous solution

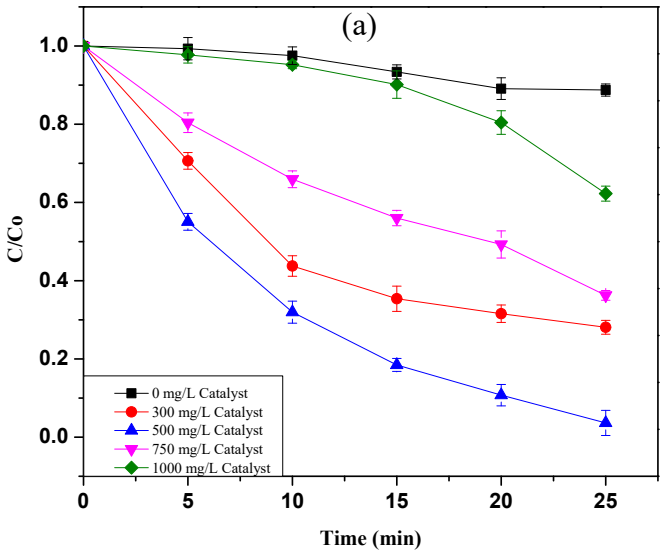
(a)
C/Co
Time (min)
0 mg/L Catalyst
300 mg/L Catalyst
500 mg/L Catalyst
750 mg/L Catalyst
1000 mg/L Catalyst

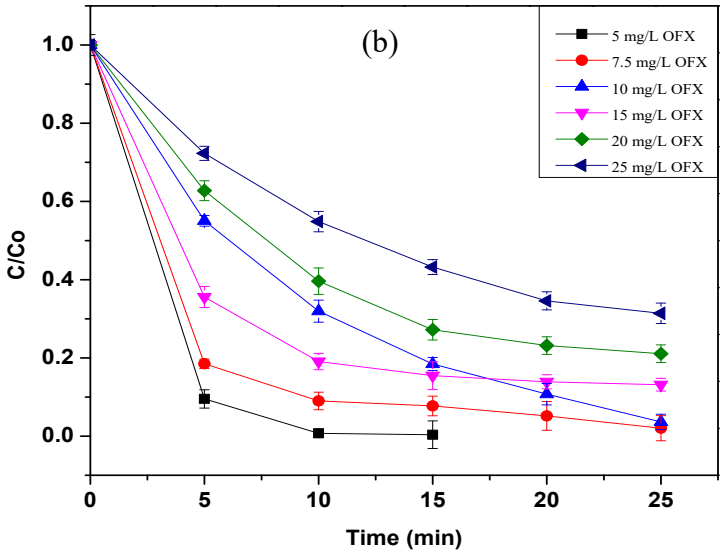
(b)
C/Co
Time (min)
5 mg/L OFX
7.5 mg/L OFX
10 mg/L OFX
15 mg/L OFX
20 mg/L OFX
25 mg/L OFX

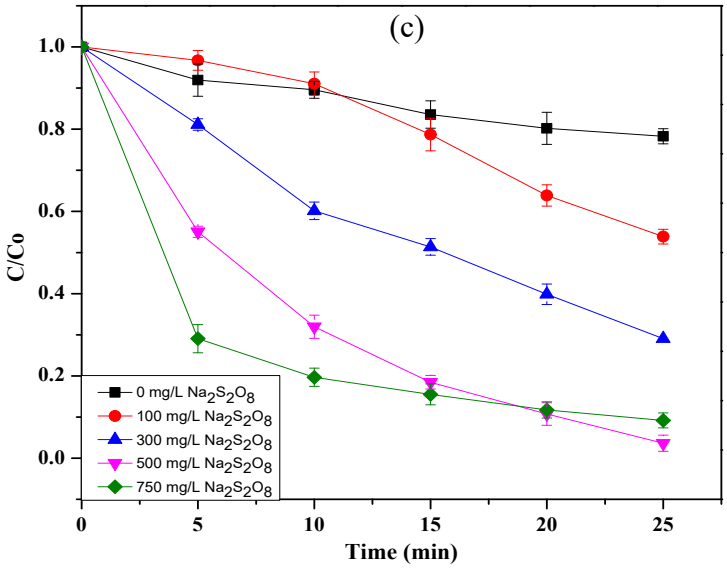

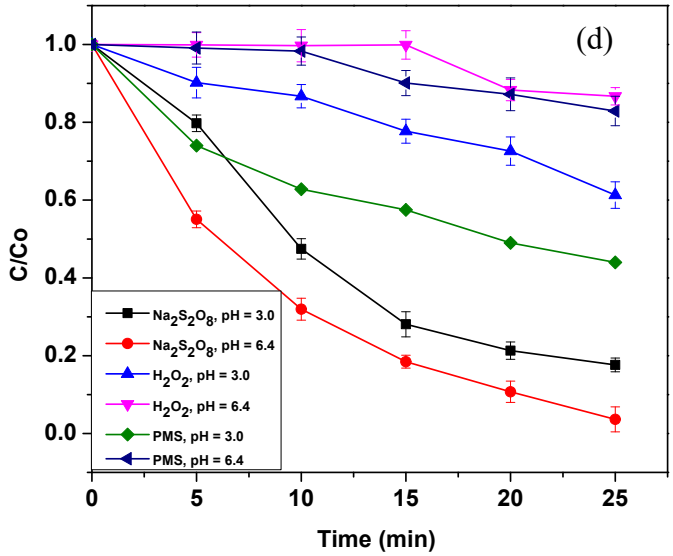

Figure S12. Effects of (a) photocatalyst dosage, (b) OFX concentration, (c) $Na_2S_2O_8$ concentration, and (d) oxidant on the photocatalytic removal efficiency of OFX (n = 3)

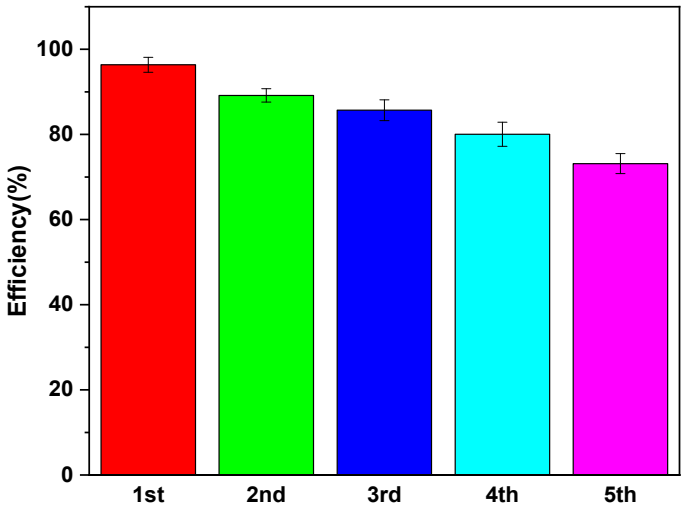

Figure S13. The degradation of OFX after 5 cycles of the photocatalytic experiment (n = 3)

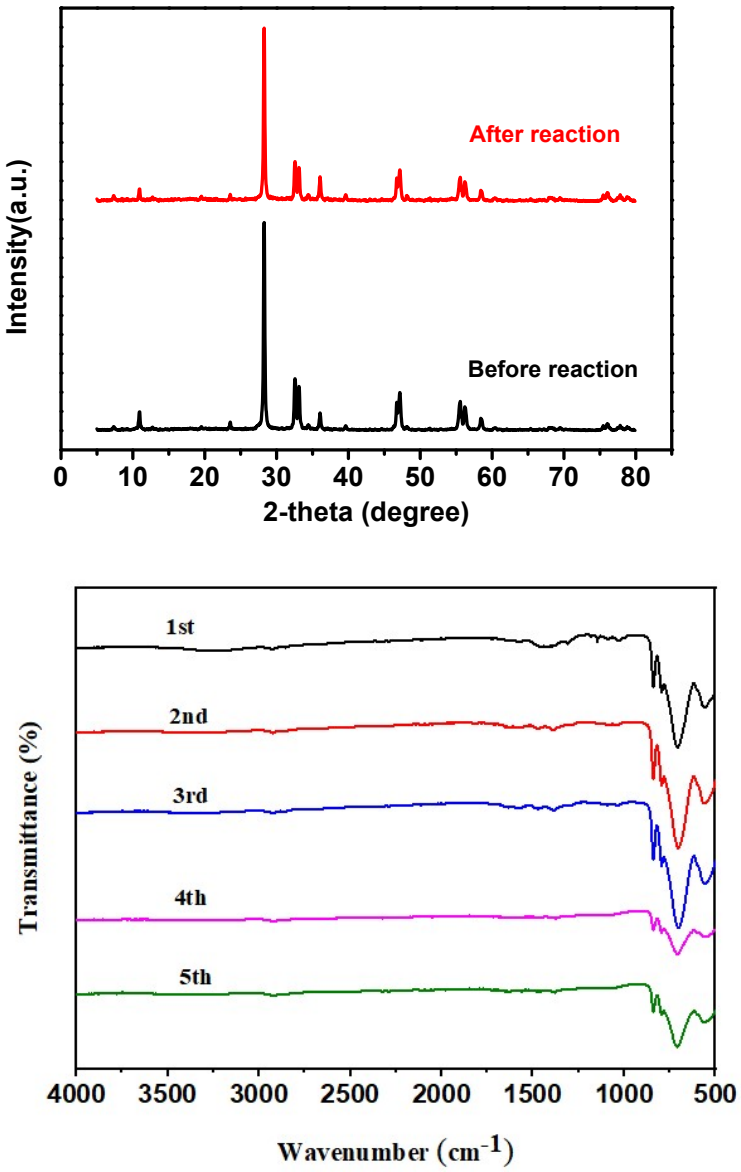

Figure S14. (a) XRD patterns of the BIZ material before and after five cycles of experiment and (b) FTIR spectra of BIZ material after each cycles of experiment

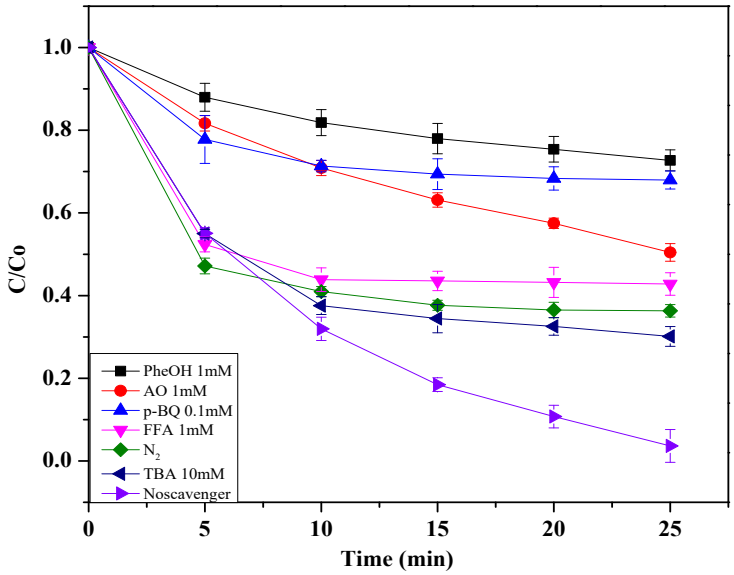

Figure S15. Effect of scavengers on the photocatalytic removal efficiency of OFX (n = 3)

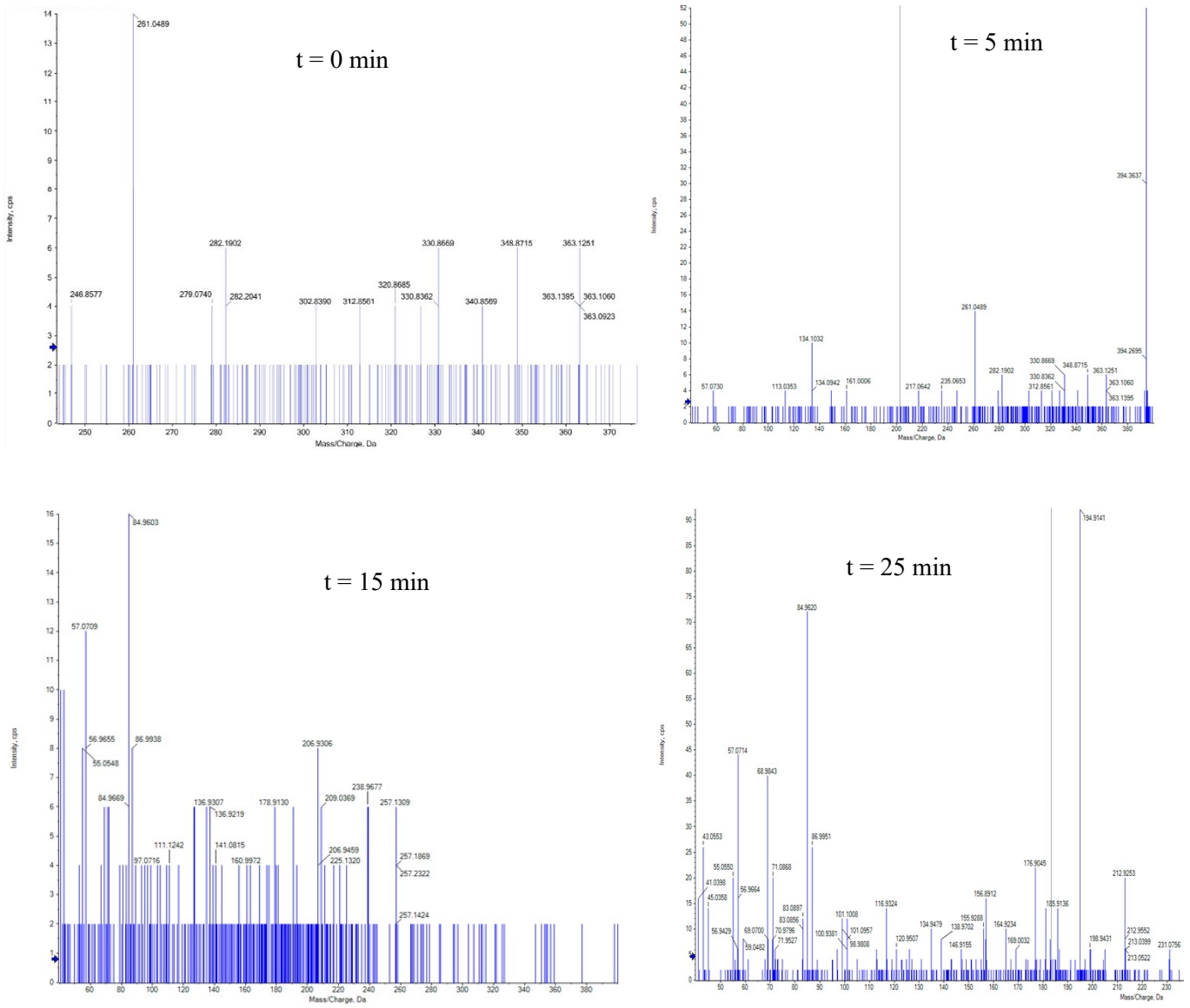

Figure S16. MS results of OFX solution during the reaction time